Phys. Med. Biol. **45** (2000) 1071–1083. Printed in the UK PII: S0031-9155(00)08732-7

Investigation of a large-area phased array for focused ultrasound surgery through the skull

G T Clement, Jason White and Kullervo Hynynen
Brigham & Women's Hospital, Harvard Medical School, 75 Francis Street, Boston, MA 02115, USA

Received 14 October 1999, in final form 31 January 2000

Abstract. Non-invasive treatment of brain disorders using ultrasound would require a transducer array that can propagate ultrasound through the skull and still produce sufficient acoustic pressure at a specific location within the brain. Additionally, the array must not cause excessive heating near the skull or in other regions of the brain. A hemisphere-shaped transducer is proposed which disperses the ultrasound over a large region of the skull. The large surface area covered allows maximum ultrasound gain while minimizing undesired heating. To test the feasibility of the transducer two virtual arrays are simulated by superposition of multiple measurements from an 11-element and a 40-element spherically concave test array. Each array is focused through an *ex vivo* human skull at four separate locations around the skull surface. The resultant ultrasound field is calculated by combining measurements taken with a polyvinylidene difluoride needle hydrophone providing the fields from a 44-element and a 160-element virtual array covering 88% and 33% of a hemisphere respectively. Measurements are repeated after the phase of each array element is adjusted to maximize the constructive interference at the transducer's geometric focus. An investigation of mechanical and electronic beam steering through the skull is also performed with the 160-element virtual array, phasing it such that the focus of the transducer is located 14 mm from the geometric centre. Results indicate the feasibility of focusing and beam steering through the skull using an array spread over a large surface area. Further, it is demonstrated that beam steering through the skull is plausible.

(Some figures in this article appear in black and white in the printed version.)

1. Introduction

Focused ultrasound has the demonstrated ability to function as an effective tool for the non-invasive treatment of a wide range of disorders (ter Haar 1999). Despite this success, high attenuation and scattering properties of bone have limited ultrasound treatment to areas that can be accessed without bone penetration. This poses a particular problem for brain disorders since transcranial ultrasound propagation is unavoidable if the procedure is to remain non-invasive. In recent experiments where a section of the skull bone is surgically removed, focused ultrasound has been used to destroy deep tissue, close blood vessels (Hynynen *et al* 1996), activate drugs (Umemura *et al* 1989) and open the blood–brain barrier. (Vykhodtseva *et al* 1995) However, the need for this complicated cranial procedure has inhibited clinical studies involving the use of ultrasound in the brain.

The risk and expense incurred by removal of skull bone could be avoided by a procedure that safely and accurately transmits ultrasound energy through the skull. It has been proposed (Fry 1977) that such a procedure could be achieved using an ultrasound transducer array to offset distortion caused by skull inhomogeneities, allowing ultrasound to focus at appropriate points without excess heating at the brain–skull interface. Advances in transducer array technology have prompted proposals for both mildly invasive (Thomas and Fink 1996) and non-invasive techniques (Sun and Hynynen 1999). A procedure of this type is contingent upon a reliable model for predicting the physical response of the skull to sonication. For example, a prediction of the location and size of the focal region could be made from knowledge of the position, thickness, orientation and structure of the skull and brain; all quantities that could be obtained *in vivo* using MRI or other non-invasive diagnostic methods.

The predominant control factor for determining the ultrasound focus is the acoustic phase (Smith *et al* 1986, O'Donnell and Flax 1988). Experimental studies (Hynynen and Jolesz 1998) have shown that it is possible to reconstruct the focus inside an *ex vivo* human skull by manual adjustment of a transducer array's driving phases. In practice, however, the phased signal would have to produce a significant acoustic pressure at the ultrasound focus without excess pressure in other regions, including the skull surface. To meet this requirement a large phased array has been proposed (Sun and Hynynen 1999) that would distribute the acoustic power over the skull surface while still allowing phase control.

The present study examines the experimental feasibility for a large array to focus ultrasound through the skull without creating damaging pressure levels outside the focal region. The study considers a 44-element array and a 160-element virtual array, each constructed through the summation of smaller test arrays placed around the skull. In this context the virtual array refers to the hypothetical transducer comprising smaller transducers. The experiment is performed using a human skull bone placed in water between a transducer test array and a needle hydrophone. The ultrasound waveform is measured over a planar area and at each location the acoustic phase is determined using the temporal Fourier transform of the received waveform at the transducer's driving frequency. Comparisons of the reconstructed pressure field are made with and without phase correction. For reference, the field is also measured without a skull in place. The phasing procedure is similar to that used by Hynynen and Jolesz (1998), but employs the superposition of the four locations to predict the response of a large-area transducer. The method demonstrates the ability of the array to correct for distortion, while increasing gain in the target area.

The feasibility of both mechanical and electronic beam steering through the skull is also demonstrated. Mechanical translation to a new position is performed by physically shifting the skull over a distance of 15 mm and repeating the above measurement procedure. To emulate electronic beam steering of the 160-element array, four unique beam patterns were developed corresponding to the relative positions of the transducer as described in section 2.

2. Materials and methods

Two focused transducer arrays are used in the study. The first transducer is shown in figure 1(*a*) to consist of an air-backed 0.665 MHz focused piezoceramic fully sectioned into 11 equal area elements: a 10-sided centre element surrounded by 10 elements that extend to the outer edge of the transducer. The diameter of the array is 10 cm and the radius of curvature is 8 cm. The second transducer is a focused air-backed 0.510 MHz array, composed of 64 square-cut elements arranged as shown in figure 1(*b*). Each element is approximately 1 cm^2. As indicated in the figure the experiment was performed with 40 of the elements, the maximum number allowed by our driving capabilities at this frequency. To emulate the effect of a large array, the 11-element transducer was moved to four locations over a 16 cm diameter hemisphere as depicted in figure 2, simulating a 44-element array. The four locations were located on the hemisphere at a 45° polar angle and at 90° azimuth intervals. Similarly the second transducer was moved to four locations on a 20 cm diameter hemisphere resulting in a 160-element

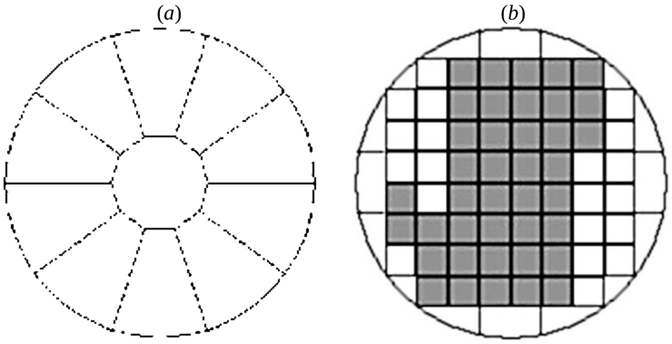

Figure 1. Geometry of transducers used to simulate a large area arrays. (*a*) 11-element array, (*b*) 64-emenent array. Gray elements are those active for the experiment.

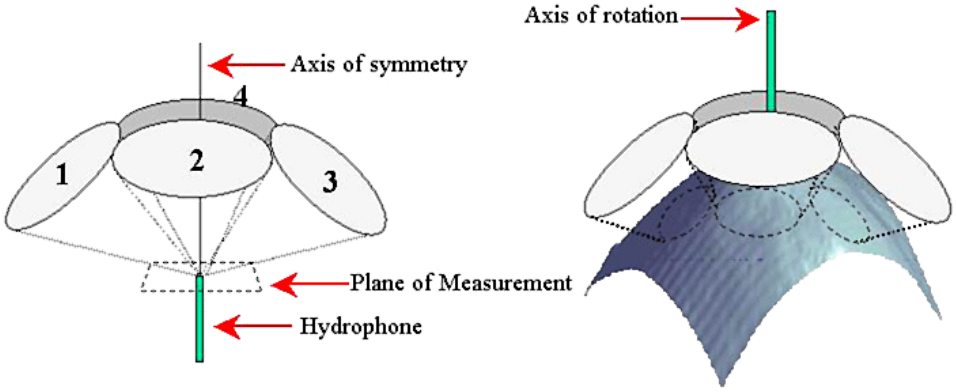

Figure 2. Diagram of the experiment. The transducer is positioned in four locations about an axis such that each position has the same geometric focus. For measurement a hydrophone is scanned over the dotted area indicated as 'plane of measurement' (left). In practice it is more practical to rotate a skull about the axis while keeping the transducer stationary (right).

virtual array. The 11-element array covers 22% of the hemisphere area it was revolved around, resulting in 88% coverage overall. The 40-elements cover 8.4% of its hemisphere of rotation so that the combined locations cover 33% of the area.

The transducer signals are generated by a phased array driving system manufactured in-house. The amplifier is equipped with phase feedback for increased control. Individual channels of the arrays are equipped with impedance matching circuitry, matching the channel to electrical resonance at 50 Ω, to ensure maximum power output to the transducer. Forward and reflected powers supplied by the driving system are monitored by an internal power meter.

Measurements are conducted in a tank filled with degassed deionized water and padded with rubber to inhibit reflections from the tank walls. A 0.5 mm diameter (Precision Acoustics, UK) polyvinylidene difluoride (PVDF) hydrophone is positioned normal to the axis of symmetry of each virtual array. The hydrophone is moved to arbitrary positions in the tank using a stepping-motor-controlled Parker 3D positioning system. Hydrophone response is sent through a Precision Acoustics pre-amp into an amplifier (Preamble Instruments, Oregon, model 1820) and recorded by a digital oscilloscope (Tektronix, Oregon, model 680). Both the scan position and the data acquisition are computer controlled. The hydrophone signal is downloaded to a PC and Fourier transformed to obtain the amplitude phase of the resonant frequency. The acoustic amplitude and phase as a function of position are obtained by placing the hydrophone along the axis of symmetry 80 mm from the hemisphere of the 44-element virtual array and 100 mm from the 160-element array. The field is measured over a 20 mm^2 area at intervals of 0.4 mm, for a total of 2500 points in the plane.

A measurement is first recorded without the skull to map the field of the virtual array in water. Next a skull is placed between the hydrophone and one of the transducers and all elements are driven in phase. The skull is then actively rotated about the axis of symmetry by 90° and the planar scan is repeated. Two more rotations are performed to provide the four planar measurements of the complex acoustic field. Finally, measurement of each transducer position is repeated, this time with the array elements manually adjusted to radiate the phase they displayed at the geometric focus before the skull was introduced.

The resultant field in water is calculated by combining the scans of the four individual transducer positions. The data sets are stored in square matrices which are rotated by 0°, 90°, 180° and 270° respectively to properly align their field orientations. Calculation of the acoustic pressure field produced by the elements of all four positions running simultaneously was achieved by combining the planar measurements

$$p(x, y) = \sum_{n=1}^{4} P_n(x, y)\, \mathrm{e}^{\mathrm{i}\phi_n(x,y)} \tag{1}$$

where P_n and ϕ_n are respectively the amplitude and phase of the acoustic pressure due to the nth array position.

Validity of the technique is examined by directing the field from the 11-element transducer through a skull and scanning the fields (a) with all elements on, (b) with five of the elements on and the remaining elements off and (c) with the six remaining elements turned on. The second and third cases are combined using equation (1) and compared with the first scan. Similarly the 40 elements of the 64-element transducer are divided and scanned. A quantitative comparison is performed using a RMS measurement was calculated for the difference in the amplitudes

$$R = \left(\frac{\sum_{i,j}^{M,N} (P_{ij} - P'_{ij})^2}{\sum_{i,j}^{M,N} (P_{ij})^2} \right)^{1/2} \tag{2}$$

where P_{ij} is a measured amplitude point over an $M \times N$ matrix and P'_{ij} is an element of the projection.

To demonstrate the feasibility of beam steering through the skull, the 160-element virtual array focus is directed away from its initial position relative to the skull by both mechanically moving the array and by electronic beam steering. Mechanical movement is achieved by moving the skull a distance of about 15 mm relative to the axis of symmetry and repeating the experiment as above but now rotating the skull about its new position. To investigate electronic shifting, the beam is first measured without a skull. Four unique focal locations are required corresponding to a single location relative to the rotated skull. The phase of each amplifier channel is recorded and an area near the new focal location scanned. Next the skull is placed in the tank and the beam patterns are repeated to construct the uncorrected field. Finally, the phase is manually corrected at the shifted focal location within the skull and the fields are again recorded.

Two *ex vivo* human calvaria fixed in formaldehyde were used in the study, referred to hereinafter as SK1 and SK2. Based on a previous study (Fry and Barger 1978) the acoustic sound speeds and attenuation properties of the internal skull structure are assumed to be similar to that of a fresh skull. Therefore phaseshifts through the fixed skull are also expected to be similar.

3. Results

3.1. Comparison of combined and direct fields

Demonstration of the approach was performed with the 11-element transducer and 40 elements of the 64-element transducer. Figure 3(*a*) shows the acoustic pressure amplitude resulting from six elements of the 11-element array directed through the skull. The field from the remaining five elements is shown in figure 3(*b*). The resultant pressure measurement shown in figure 4(*a*) is obtained by combining amplitude and phase data using equation (1). This measurement is compared with the field in figure 4(*b*), obtained by driving all 11 elements simultaneously. The RMS difference was calculated from equation (2) to be 0.042 over the area. Improved agreement between the combined and directly measured fields was found using the 40-element transducer. The RMS difference in this case was found to be 0.0081.

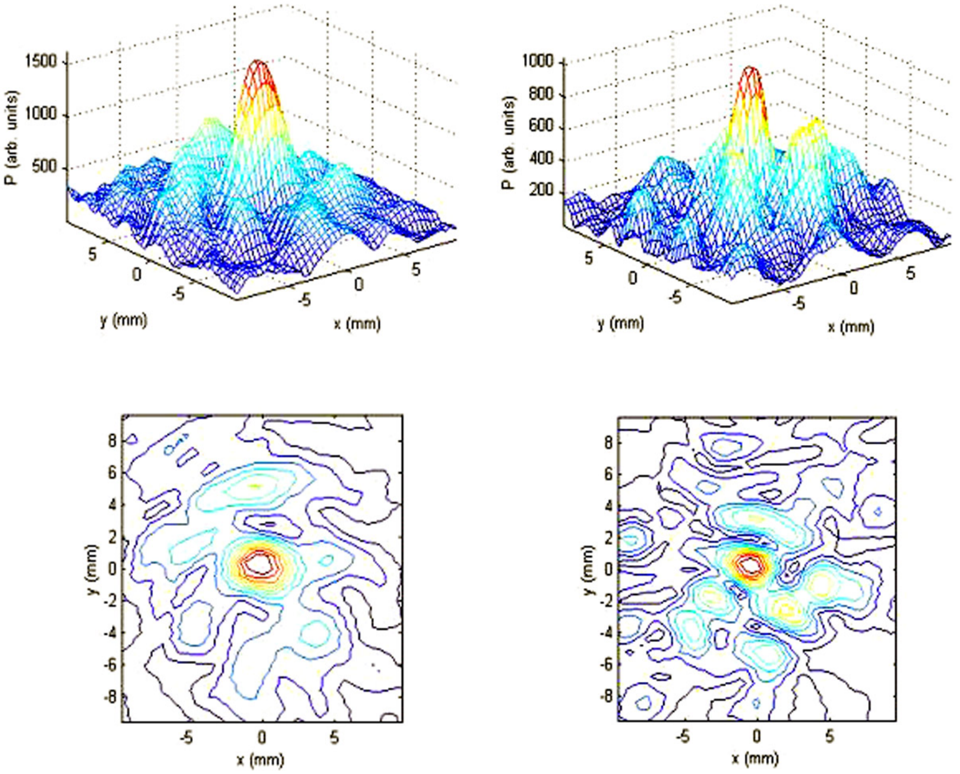
(*a*) (*b*)

Figure 3. (*a*) Pressure measurement of elements 1–32 of a 64-element array focused through a human skull (above) and its corresponding contour (below). The pressure scale is in uncalibrated (arbitrary) units. (*b*) Scan of elements 33–64.

3.2. 44-element array

The 11-element array was driven at the four symmetric transducer locations and the amplitudes and phase recorded as a function of position about the geometric centre of the assembly. Contour plots of the acoustic pressure amplitude after passing through skull SK1 are presented in figures 5(*a*)–5(*d*). At each of the four positions, individual elements of the array were then

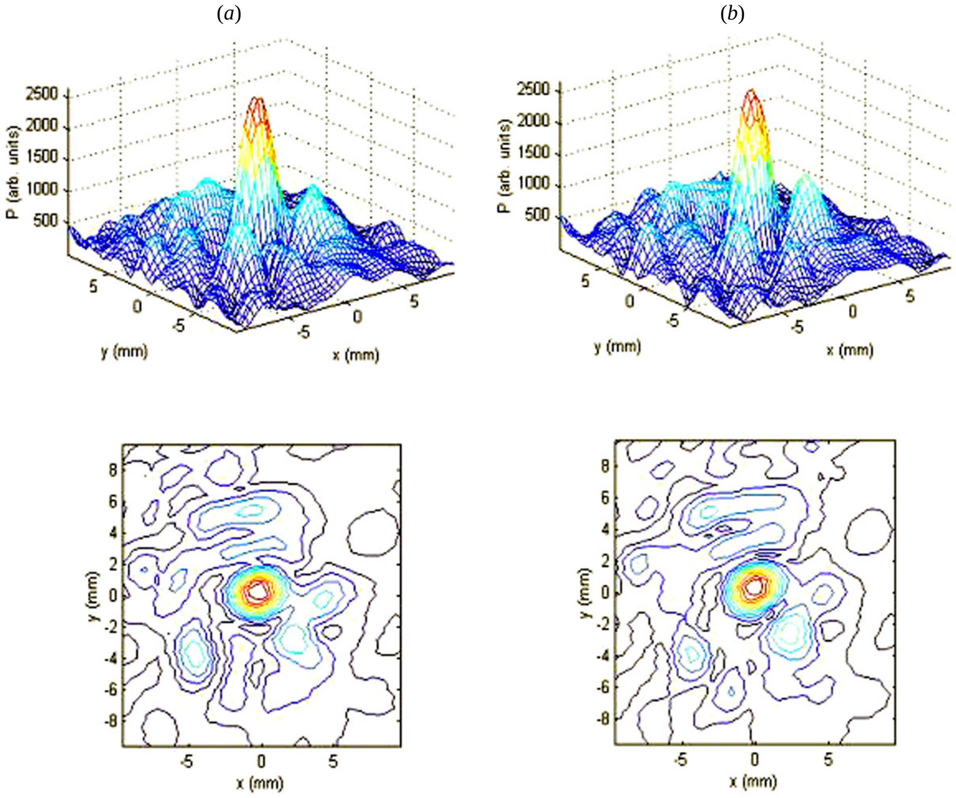

Figure 4. (*a*) Pressure field from the combination of elements 1–32 with elements 33–64 (above) and its corresponding contour (below). The pressure scale is in uncalibrated units. (*b*) Direct measurement taken by driving elements 1–64 simultaneously.

shifted in phase so that all elements exhibited the same phase at the geometric centre and the scans were then performed again. The resulting amplitudes are displayed in figures 6(*a*)–6(*d*) showing significant improvement over their uncorrected counterparts in figure 5.

The acoustic power due to a 44-element array was calculated using equation (1), where the power is proportional to the modulus of the pressure squared. The uncorrected field through SK1 is shown in figure 7(*a*) and the corrected field in figure 7(*b*). The field in water without the skull is shown in figure 7(*c*). Phase correction successfully reproduced a sharp peak at the geometric centre of the array while reducing the surrounding side-lobes. In figure 8 a radial cross section of the corrected field is compared with the field taken in water without the skull. Expected reflection and attenuation by the skull has lowered the peak acoustic pressure to less than 26% of the value in water, representing a -5.85 dB drop in power. However, the full width at half maximum (FWHM) value for the diameter of the central lobe of the acoustic pressure is 1.8 cm both with and without the skull. All grating lobes of the field measured without the skull were less than 2% of the peak power. When the field through the skull was phase corrected all side lobes were measured to be less than 15% of its peak.

Similar measurements were performed for skull SK2, which produced a reconstructed peak pressure amplitude equal to 35% of the value in water. Maximum power away from the central lobe was 3% of the peak value without the skull and 16% for the phase-corrected signal propagated through the skull.

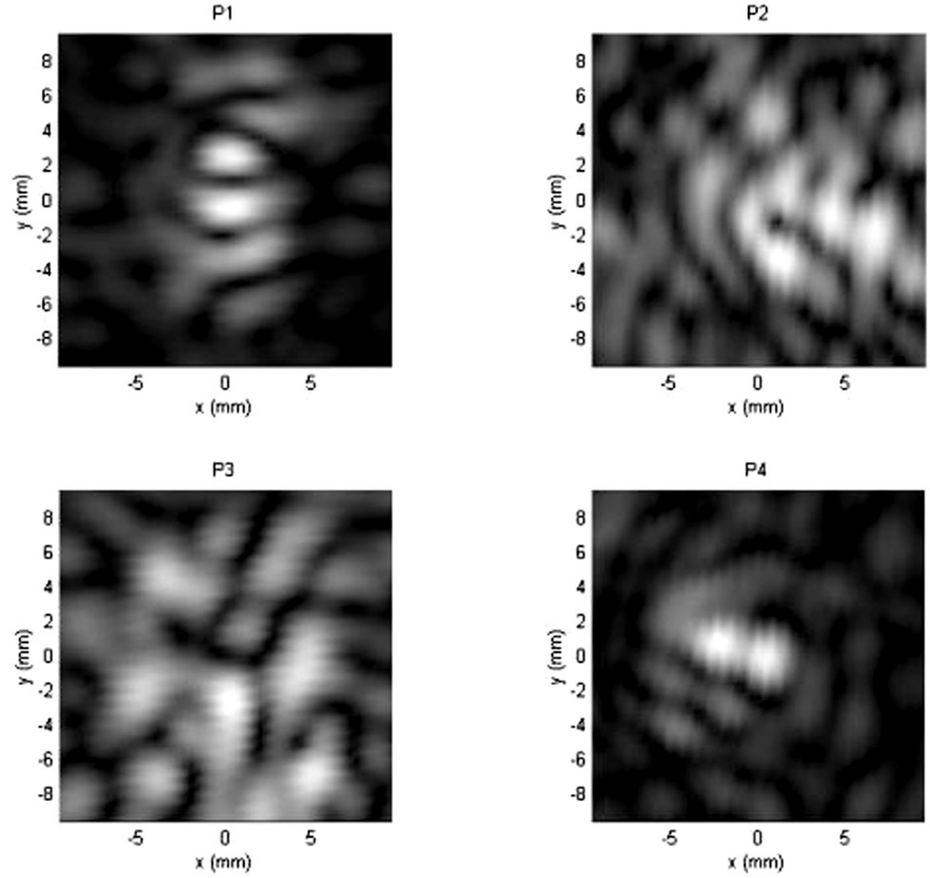

Figure 5. Pressure intensity plots of the four measured positions relative to the skull (P1–P4) with all elements driven in phase.

3.3. 160-element array

3.3.1. Centralized focus. The experiment was repeated using 40 channels of the 64-element transducer. The uncorrected acoustic power was first calculated as shown in figure 9(*a*) for skull SK1. Next the elements were manually corrected in each position and the fields were again recorded. The corrected power is displayed in figure 9(*b*), and may be compared with the power in water without a skull shown in figure 9(*c*). The uncorrected acoustic pressure had a peak amplitude equal to 26% of the peak value in water. The phase corrected measurement had a peak value equal to 42% of the peak in water.

Using SK2, peak values of 22% uncorrected and 34% phase corrected were observed. The focus without a skull had a central lobe FWHM of 1.58 mm while the power directed through the skull had a FWHM value of 1.76 mm. The peak side-lobes without the skull were 20% of the signal maximum. The focus through the skull contained peak side-lobes that were 34% of the maximum.

3.3.2. Mechanically shifted focus. The skull was moved a distance of about 15 mm normal to the 160-element array axis and the scan procedure repeated. Results are shown in figures 10(*a*)–10(*c*). The corrected value through the skull was 31% of the value without

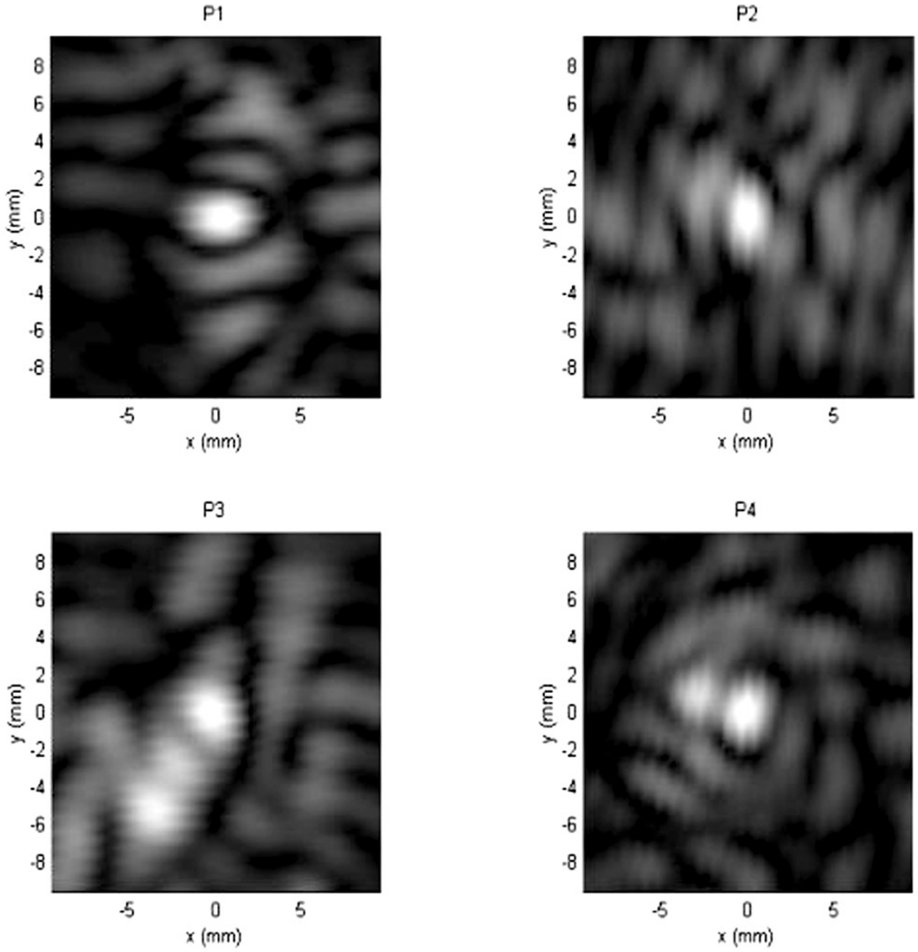

Figure 6. Pressure intensity plots of the four measured positions relative to the skull (P1–P4) after correcting the phase of each element.

the skull, corresponding to a −10 dB drop in acoustic power. The power FWHM of the central peak in water alone is 1.51 mm and the FWHM value through the skull is 1.59 mm when phase corrected. A small increase in the side-lobe amplitude was observed after transcranial propagation. The first side-lobes without the skull were 28% of the peak value, while the phase corrected field through the skull produced lobes 35% of the central peak.

3.3.3. Electronically steered focus. The driving phase of each amplifier channel was determined for the shifted focus in water, where the focus was steered to a Cartesian position (10,10) mm relative to the geometric centre. Skull SK1 was then inserted between the hydrophone and the transducer and the resulting field within the skull was measured without further phase changes. The resulting amplitude from the 160-element virtual array at this intended focus is presented in figure 11(*a*). The procedure was repeated with phase correction and is seen in figure 11(*b*) to significantly improve the focus. The diameter of the phase corrected beam is similar to that of the beam in water shown in figure 11(*c*). The uncorrected field was found to have a peak amplitude equal to 18% of the maximum value measured in

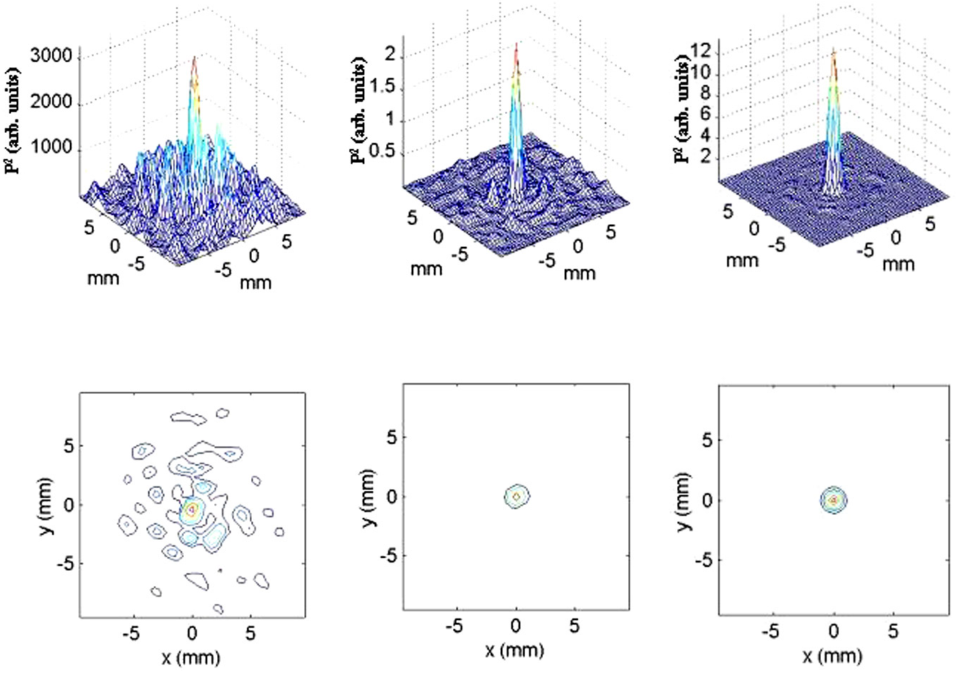
(*a*) Uncorrected field (*b*) Phase-corrected field (*c*) Field in water

Figure 7. (*a*) Pressure-squared values resulting from combination of four 11-element array measurements through a human skull to produce the field due to a 44-element array (above) and its corresponding contour plot (below). (*b*) Similar measurements taken after phase correction. (*c*) The combined field measured without a skull.

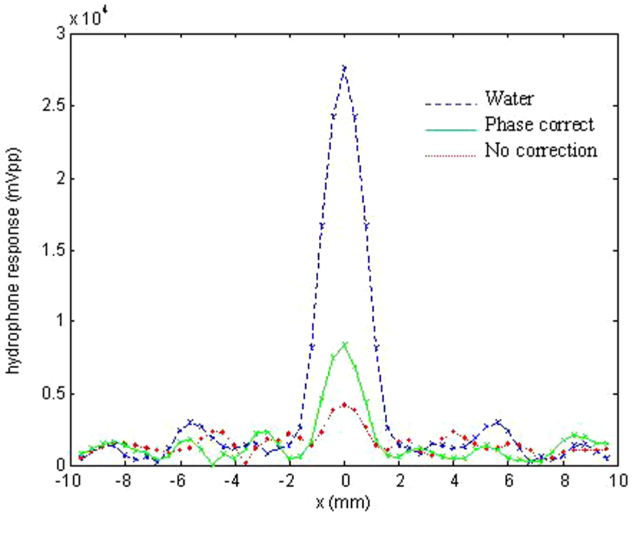

Figure 8. A radial cross section of the phase corrected pressure field (solid), the uncorrected field (dotted), and the field in water (dashed).

water. With phase correction, the peak value was improved to 34%. The power FWHM value was 1.50 mm without the skull and 1.55 mm phase corrected through the skull.

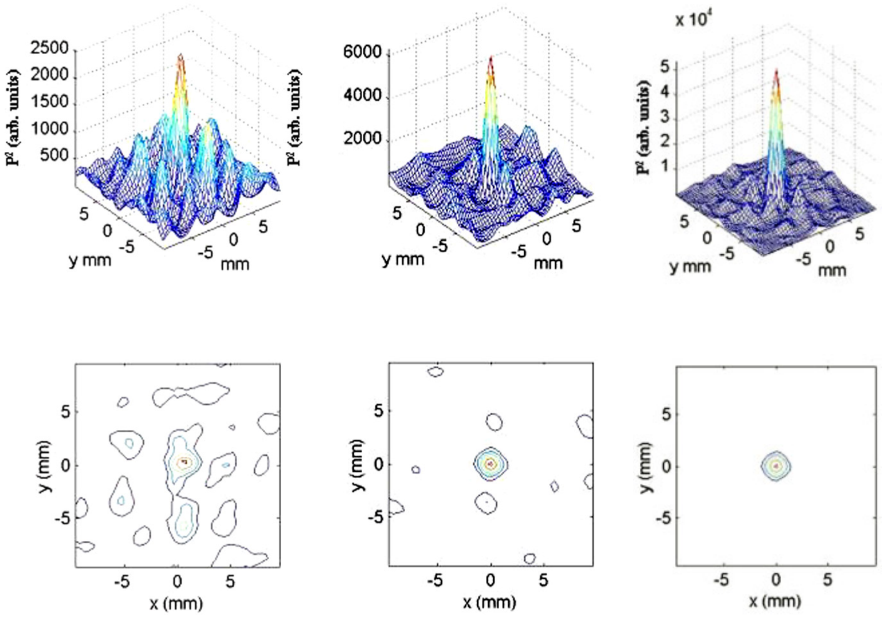
(*a*) Uncorrected field (*b*) Phase-corrected field (*c*) Field in water

Figure 9. (*a*) Pressure-squared values resulting from combination of four 40-element array measurements through a human skull to produce the field due to a 160-element array (above) and its corresponding contour plot. (*b*) Similar measurements taken after phase correction. (*c*) The combined field measured without a skull.

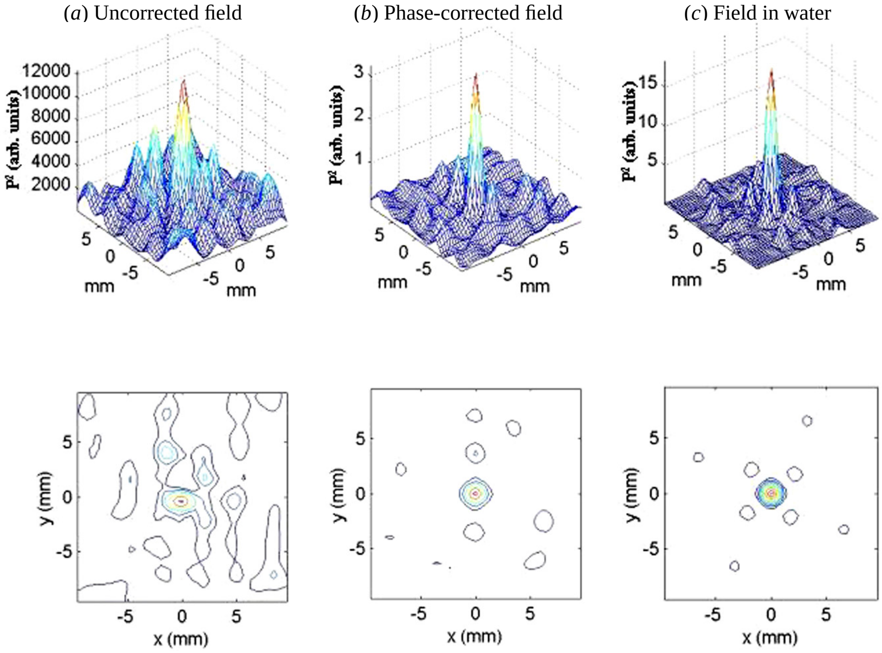
(*a*) Uncorrected field (*b*) Phase-corrected field (*c*) Field in water

Figure 10. (*a*) Pressure-squared values resulting from combination of four 40-element array measurements through a human skull after shifting the transducer 15 mm relative to the skull. (*b*) Similar measurements taken after phase correction. (*c*) The combined field measured without a skull.

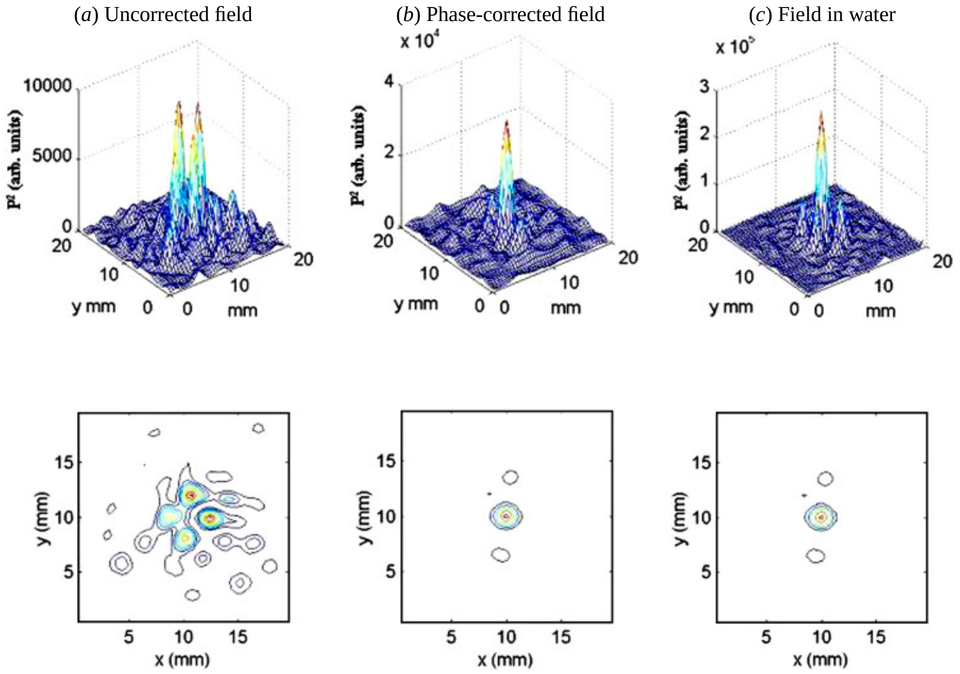
(*a*) Uncorrected field (*b*) Phase-corrected field (*c*) Field in water

Figure 11. (*a*) Pressure-squared values resulting from combination of four 40-element array measurements through a human skull with a focus electronically shifted 10 mm × 10 mm off axis. (*b*) Similar measurements taken after phase correction. (*c*) The combined field measured without a skull.

4. Discussion

Construction of virtual array fields through the skull is designed to assist in the development of a full hemisphere array for transskull therapeutic applications. Non-invasive treatment of brain disorders requires an array that can produce an appreciable acoustic pressure field in a small region within the brain while leaving surrounding regions undamaged. In addition, temperature elevation induced through attenuation while travelling through the skull must be minimized. Our approach to these problems is to distribute the propagation region over a large area of the skull surface while controlling the acoustic phase by sectioning the transducer into individual elements. The large area allows the overall acoustic intensity at the skull to be reduced while sectioning permits phase control over discrete regions.

In practice it would be advantageous to phase correct for field distortion using as few elements as possible thereby simplifying the procedure, lowering cost and reducing the time required to calculate the phasing of each element for the transducer. Expanding the elements of the 44-element array over an entire hemisphere would produce a 50-element array. Results of the virtual array tests shown in figure 7 suggest that this surprisingly small number of elements is sufficient for phase correction at the focus at 0.664 MHz. However, it is not possible to effectively move the beam through electronic phasing with so few elements. Beam steering by mechanical shifting of the transducer may be possible with the 44-element array but was not studied due to the small (80 mm) radius of curvature of the transducer. The limited size prevented the skulls—which were both nearly 160 mm across—from being moved inside the hemisphere.

The 160-element array is demonstrated to provide sufficient control for both electronic and mechanical beam steering. Results from the electric phaseshifting shown in figure 11 indicate that a beam can be successfully shifted 14 mm from its geometric focus suggesting that the focus could be moved in a volume $20 \times 20 \times 10$ mm^3 under the conservative assumption of a 10 mm effective range backward toward the source in the axial direction not studied here. This volume would be even larger if electronic shifting were combined with mechanical movement of the transducer, such as that shown in figure 8. The maximum mechanical motion tested with our system was 15 mm, translating to a volume of at least $30 \times 30 \times 30$ mm^3 in the middle of the brain. Tissue volumes deep in the brain could be treated using this technique. Target volumes closer to the brain surface would require an array with additional elements to provide a larger range of beam steering.

Acoustic pressure after phase correction and propagation through the skull was found to range from 26% to 42% of the value in water. These values may be compared with ideal values calculated using a normally incident ultrasound wave propagating through a homogeneous skull. Using an amplitude attenuation coefficient of 50 Np m^{-1} (Goss *et al* 1979) and a *pressure* transmission coefficient we measured to be 0.73, values of 40% to 65% were calculated over a range of skull thicknesses from 2 mm to 12 mm. Additional loss observed in each of the phase-corrected experimental measurements can be attributed to uncorrected scattering of the ultrasound as well as reflection due to oblique incidence upon the skull and internal skull structure.

5. Conclusions and future work

Overall results indicate that it is possible to correct for distortion due to transskull propagation over a large area using only adjustment of the driving phase. Further, it is demonstrated that both mechanical translation of the source and electronic beam steering through the skull can be achieved. Use of both electric steering and mechanical shifting in combination could permit the treatment in an appreciable volume ($> 30 \times 30 \times 30$ mm^3) in the centre of the brain using fewer than 200 elements. Future investigation will concentrate on the production of a full hemisphere-shaped array for transskull therapy. Combined with an accurate phase prediction model and a diagnostic method such as MRI to monitor treatment (Cline *et al* 1994), this array could provide a completely non-invasive tool for the treatment of brain disorders.

Acknowledgments

This work was supported by TxSonics Inc. and grant CA 76550 from the National Institutes of Health. The authors would like to thank Samuel Kennedy and Cynthia A McDermott of the Harvard Medical School for their assistance in obtaining the calvaria samples.

References

Cline H E, Hynynen K, Hardy C J, Watkins R D, Schenck J F and Jolesz F A 1994 MR temperature mapping of focused ultrasound surgery *Magn. Reson. Med.* **31** 628–36

Fry F J 1977 Transkull transmission of an intense focused ultrasonic beam *Ultrasound Med. Biol.* **3** 179–84

Fry F J and Barger J E 1978 Acoustical properties of the human skull *J. Acoust. Soc. Am.* **63** 1576–90

Goss S A, Frizzell L A and Dunn F 1979 Ultrasonic absorption and attenuation in mammalian tissues *Ultrasound Med. Biol.* **5** 181–6

Hynynen K, Colucci V, Chung A and Jolesz F 1996 Noninvasive arterial occlusion using MRI-guided focused ultrasound *Ultrasound Med. Biol.* **22** 1071–7

Hynynen K and Jolesz F A 1998 Demonstration of potential non-invasive ultrasound brain therapy through an intact skull *Ultrasound Med. Biol.* **24** 275–83

O'Donnell M and Flax S W 1988 Phase aberration measurements in medical ultrasound: human studies *Ultrason. Imaging* **10** 1–11

Smith S W, Trahey G E and von Ramm O T 1986 Phased array ultrasound imaging through planar tissue layers *Ultrasound Med. Biol.* **12** 229–43

Sun J and Hynynen K 1999 The potential of transskull ultrasound therapy and surgery using the maximum available skull surface area *J. Acoust. Soc. Am.* **105** 2519–27

ter Haar G 1999 Therapeutic ultrasound *Eur. J. Ultrasound* **9** 3–9

Thomas J-L and Fink M A 1996 UItrasonic beam focusing through tissue inhomogeneities with a time reversal mirror: application to transskull therapy *IEEE Trans. Ultrason. Ferroelectr. Freq. Contr.* **43** 1122–9

Umemura S A, Yumita R and Nishigaki R 1989 Sonochemical activation of hematoporphyrin: a potential modality for cancer treatment *IEEE 1989 Ultrasonics Symp. Proc.* pp 955–60

Vykhodtseva N I, Hynynen K and Damianou C 1995 Histologic effects of high intensity pulsed ultrasound exposure with subharmonic emission in rabbit brain *in vivo Ultrasound Med. Biol.* **21** 969–79